Enhanced resonant backscattering of light from quantum-well excitons

Vincenzo Savona, Erich Runge, and Roland Zimmermann
Institut für Physik der Humboldt-Universität zu Berlin, Hausvogteiplatz 5-7, D-10117 Berlin, Germany
(Received 6 April 2000)

The angle-dependent resonant Rayleigh scattering of light from excitons in a disordered quantum well is studied theoretically. An enhancement of the scattered intensity peaked on the backscattering direction is predicted, for values of the parameters corresponding to realistic GaAs/AlGaAs heterostructures. It is shown that this effect can be isolated by measuring the differential enhancement between two different scattering directions. An analysis in terms of perturbation theory provides a simple analytical approximation of the measurable quantity.

In recent years, the influence of structural disorder on the optical properties of excitons in semiconductor heterostructures has become the object of numerous experimental and theoretical investigations. In addition to improving our understanding of the physics of excitons, these studies are also part of a much broader perspective, aiming at the systematic study of the general properties of disordered systems through the investigation of the optical response of semiconductors. Of particular interest is the resonant Rayleigh scattering (RRS) mechanism,[1–9] namely, the resonant light scattering into all directions due to the localization of the exciton center of mass wave functions. RRS measurements using interferometric[3,4] or speckle-resolved techniques[7] proved to be a powerful tool for the study of dephasing processes in semiconductors. In addition, time-resolved RRS measurements[9] and a microscopic RRS model[8] have given access to the statistics of energy-level distances characterizing the exciton center-of-mass motion.

A general property of disordered systems consists in the enhanced backscattering (EBS) of a wave propagating through the disordered medium. The origin of this phenomenon lies in the time-reversal invariance of the system, which holds generally in absence of a magnetic field. The same mechanism is responsible for the weak localization of a quantum-mechanical particle in a disordered potential. The EBS of light has been observed in several light-scattering experiments in diffuse media,[10] where the angular width of the EBS peak is related to the mean free path characterizing the multiple scattering process. In the case of electron transport in metals,[11] the EBS is responsible for the scaling behavior of the low-temperature conductivity and, in three-dimensional systems, of the metal-insulator transition. In semiconductors, the basic physics governing the EBS has been taken into account by Hanamura[12] in conjunction with Coulomb interaction to describe the generation of conjugated waves in four-wave mixing measurements. However, in this work the single-scattering contribution to EBS which we show to be dominant, was neglected. Apart from this single application, the relevance of EBS in the framework of RRS measurements on quantum wells has never been addressed, despite the generality of the phenomenon.

In this work we evaluate the resonant EBS of light at the exciton transition in a quantum well with in-plane disorder. We demonstrate that, in a realistic experimental situation, the EBS can be evidenced in a differential enhancement measurement, where the scattered intensities along and across the plane of incidence are compared. By means of a perturbation theory, we provide an analytical expression of EBS which satisfactorily accounts for the numerical results.

In what follows we adopt the theory of resonant Rayleigh scattering of excitons in quantum wells that we have recently developed in Ref. 8. It is assumed that the disorder affects the exciton center-of-mass motion giving rise to localized exciton eigenstates. The microscopic exciton polarization $P(\mathbf{R},t)$ is proportional to the exciton center-of-mass wave function. An incoming electromagnetic wave drives the exciton polarization which propagates according to the Schrödinger equation

$$-i\hbar\partial_t P(\mathbf{R},t)=\left(-\frac{\hbar^2}{2M}\Delta_{\mathbf{R}}+V_{\mathbf{R}}+\hbar\omega_x\right)P(\mathbf{R},t)+i\,\gamma P(\mathbf{R},t)+\mu E_{in}(\mathbf{R},t). \quad (1)$$

Here, $\hbar\omega_x$ is the average exciton energy which we set to zero for simplicity, and γ is the homogeneous damping term, accounting for radiative recombination and dephasing processes. The potential $V_{\mathbf{R}}$ describes the effect of disorder on the exciton center-of-mass motion. Within our model, $V_{\mathbf{R}}$ is a randomly distributed spatially correlated potential characterized by

$$\langle V_{\mathbf{R}} V_{\mathbf{R}'}\rangle=\sigma^2 f_{\mathbf{R}-\mathbf{R}'}, \quad (2)$$

where σ is the average amplitude of fluctuations and $f_{\mathbf{R}}$ is a correlation function with $f(0)=1$. Here the angular brackets denote an average over the statistical ensemble. For the present calculation, we take a Gauss correlation $f_{\mathbf{R}}=\exp(-R^2/2\xi^2)$, where ξ is the disorder correlation length.

The resonantly scattered field is, in the far-field limit, proportional to the Fourier transform of $P(\mathbf{R},t)$. We are interested in the frequency- and angle-resolved scattered intensity defined as $I_{\mathbf{k}_{in}}(\mathbf{k}_{out},\omega)\propto|P_{\mathbf{k}_{in}}(\mathbf{k}_{out},\omega)|^2$, where

$$P_{\mathbf{k}_{in}}(\mathbf{k}_{out},\omega)=\int d\mathbf{R}\int dt P_{\mathbf{k}_{in}}(\mathbf{R},t)e^{-i(\omega t-\mathbf{k}_{out}\cdot\mathbf{R})}, \quad (3)$$

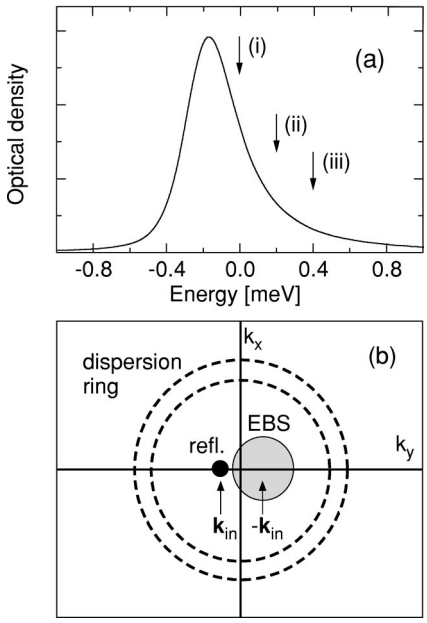

FIG. 1. (a) Computed exciton optical density. The labeled arrows refer to the three energy values considered in Fig. 2. (b) Sketch of the different contributions to the RRS intensity in the $\mathbf{k}_{out}$ plane for fixed ω. The dispersion ring (dashed) represents the exciton resonance, the black spot positioned at $\mathbf{k}_{in}$ corresponds to the reflected signal, while the shaded circle centered at $\mathbf{k}_{out}=-\mathbf{k}_{in}$ represents the broad EBS feature.

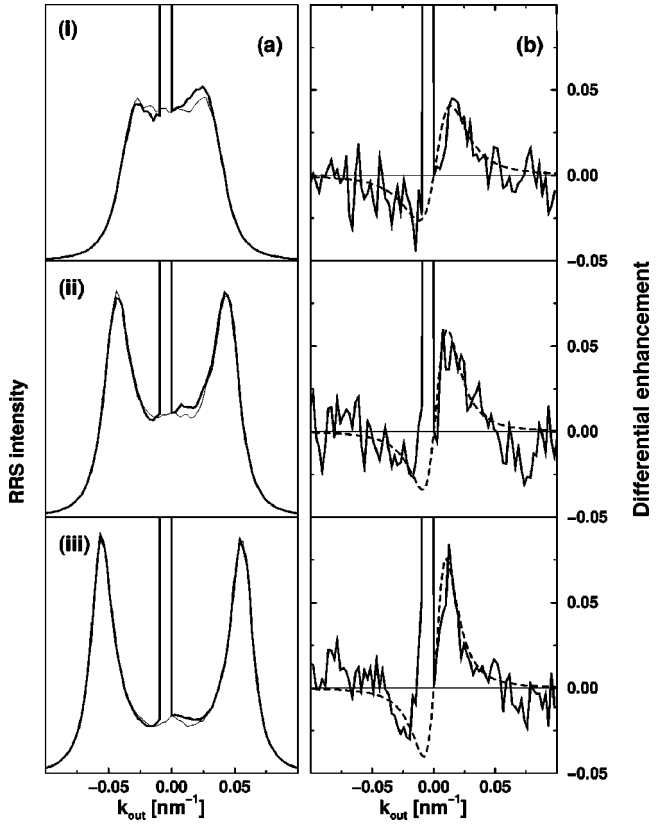

FIG. 2. (a) RRS intensity as a function of $\mathbf{k}_{out}$ for $\mathbf{k}_{in}=-0.005$ nm^{-1} and $\hbar\omega=0$ (i), $\hbar\omega=0.2$ meV (ii), and $\hbar\omega=0.4$ meV (iii), as indicated by the corresponding arrows in Fig. 1. $\mathbf{k}_{out}$ varies along the $\mathbf{k}_x$ direction (thick line) and along the $\mathbf{k}_y$ direction (thin line). (b) Corresponding plots of the differential enhancement Eq. (4) (full line). The dashed curves are fits obtained using the analytical result Eq. (7).

and $P_{\mathbf{k}_{in}}(\mathbf{R},t)$ is the numerical solution of Eq. (1) for an incoming short-pulse field $E_{in}(\mathbf{R},t)=\delta(t)\exp(-i\mathbf{k}_{in}\cdot\mathbf{R})$. The intensity is then averaged over several realizations of the disordered potential.

We point out that, with the exception of speckle-resolved measurements,[3,4,7] in a typical experimental setup the measured intensity is always averaged over a solid angle larger than the angular speckle size, the latter being inversely proportional to the excitation focus. Such speckle average is equivalent to a configuration average, as shown in Ref. 8. The angle-dependent features that we investigate in the present paper, however, take place over a scale much larger than the typical averaging angle. They are thus correctly described within our configuration-average approach.

The numerical results presented below are computed for $\mathbf{k}_{in}=(-0.005,0)$ nm^{-1}, defined on the (k_x,k_y) plane. The other parameters are set to $\sigma=0.5$ meV, $\xi=10$ nm, and $\gamma=35$ μeV. Figure 1(a) displays the optical density of the exciton, defined as the imaginary part of $P_{\mathbf{k}_{in}}(\mathbf{k}_{in},\omega)$, as a function of $\hbar\omega$. It corresponds to the spectral function of the exciton center-of-mass motion. In Fig. 2(a) we plot the scattered intensity $I_{\mathbf{k}_{in}}(\mathbf{k}_{out},\omega)$ as a function of $\mathbf{k}_{out}$ for three different values of ω lying on the high-energy tail of the exciton spectral function, as indicated by the arrows in Fig. 1(a). For the thick lines in Fig. 2(a), $\mathbf{k}_{out}$ is varied along the $\mathbf{k}_x$ direction while the thin lines represent the intensity for $\mathbf{k}_{out}$ varying along the $\mathbf{k}_y$ direction. The strong reflected signal shows up in the three thick curves as a sharp peak at $\mathbf{k}_{out}=\mathbf{k}_{in}$. The two peaks appearing in each plot at symmetrical positions with respect to the origin correspond to the exciton resonance, translated into $\mathbf{k}_{out}$ via the exciton dispersion $\hbar(\omega-\omega_x)=\hbar^2k_{out}^2/(2M)$. The enhanced backscattering manifests itself as a broad, small feature, centered on $\mathbf{k}_{out}=-\mathbf{k}_{in}$. By construction, the thin curves are totally symmetric, displaying the exciton-dispersion peaks, but neither the reflected nor the backscattered feature, as expected. All these features are better understood looking at a sketch of the scattered intensity on the $\mathbf{k}_{out}$ plane, as displayed in Fig. 1(b), where the reflected and backscattered peaks appear as a sharp and a broad feature centered on $\mathbf{k}_{in}$ and $-\mathbf{k}_{in}$, respectively, whereas the ring-shaped feature corresponds to the exciton dispersion. Since the backscattering enhancement appears as a rather faint feature in Fig. 2(a), we propose as a possible measurable quantity the differential enhancement, defined as

$$I_D(k,\omega)=\frac{I_{\mathbf{k}_{in}}((k,0),\omega)-I_{\mathbf{k}_{in}}((0,k),\omega)}{I_{\mathbf{k}_{in}}((k,0),\omega)+I_{\mathbf{k}_{in}}((0,k),\omega)}, \tag{4}$$

namely the fractional enhancement of the thick with respect to the thin lines in the plots of Fig. 2(a). This quantity is plotted in Fig. 2(b). Apart from the noise—originating from insufficient configuration averaging and amplified in this differential quantity—the enhanced backscattering feature is now well resolved as an overall variation of about ten percent. The EBS feature in both Figs. 2(a) and 2(b) is partially hidden by the large reflected peak which is rather broad. The width of the reflected peak is, however, not realistic in our

computations where, due to numerical limitations, we were restricted to a Gauss focus of 500 nm for the incident beam. In a typical experiment, the excitation focus is 50 μm wide and the reflected beam would be correspondingly narrower.

We give some remarks concerning the feasibility of the proposed measurement. In a typical GaAs heterostructure (index of refraction $n=3.6$) with an exciton energy of 1.5 eV, the external light cone corresponds approximately to an area of radius 0.008 nm^{-1}. Therefore, the incoming wave vector that we have assumed corresponds to an external incidence angle of about 40 degrees, and the predicted enhancement takes place entirely within the external light cone. Hence, the EBS is in principle measurable with a conventional experimental setup. As a further advantage of measuring the differential enhancement Eq. (4), we remark that such a quantity is not affected by multiple interference of the scattered light propagating through a realistic heterostructure. This effect depends on $|\mathbf{k}_{out}|$ only, and thus influences with equal weights the numerator and denominator, canceling in the ratio. The experiment that could provide a verification of our theory consists in measuring the angle-dependent intensity scattered off a quantum well structure excited by a monocromatic beam of frequency ω and incident angle θ with respect to the normal. The incident wave vector is defined by $\sin(\theta)=k_{in}c/\omega$. The intensities measured along the azimuthal direction containing $\mathbf{k}_{in}$ and along the orthogonal direction then allow a direct evaluation of the quantity Eq. (4). As mentioned above, in GaAs heterostructures, only a small interval around $\mathbf{k}_{out}=0$ can be accessed, in which, however, takes place the strongest variation of I_D, as illustrated in Fig. 2(b). A possible improvement with respect to the standard detection scheme would be the use of a *solid immersion lens*. This technique has been successfully employed in quantum wells to probe wave vectors beyond the standard external light cone.[13]

The most intuitive picture of the EBS mechanism is that of multiple scattering.[10] The enhancement is shown to be peaked at $\mathbf{q}=0$ spreading over an angle defined by $ql_0\simeq 1$, where $\mathbf{q}=\mathbf{k}_{out}+\mathbf{k}_{in}$ and l_0 is the mean free path between individual scattering events. The maximum enhancement turns out to be exactly a factor of two in the case of multiple light scattering in diffuse media,[10] due to a selection rule, valid for cross-polarized light scattering, that excludes the paths involving only one scattering event. Otherwise, in the general case, single-scattering paths contribute an additional background intensity. Despite its simplicity, this picture is only of limited use in our case, since one cannot define an individual scattering event in the case of a continuous spatially correlated disordered potential. A more formal approach consists in developing the perturbation theory for two-particle propagators, according to the standard diagrammatic technique.[14] The scattered intensity is indeed proportional to the configuration-averaged two-exciton propagator according to

$$I_{\mathbf{k}_{in}}(\mathbf{k}_{out},\omega)=\langle \mathcal{G}^{+}(\mathbf{k}_{in},\mathbf{k}_{out},\omega)\mathcal{G}^{-}(\mathbf{k}_{in},\mathbf{k}_{out},\omega)\rangle, \quad (5)$$

where $\mathcal{G}^{\pm}(\mathbf{k}_{in},\mathbf{k}_{out},\omega)$ denotes the retarded $(+)$ and advanced $(-)$ exciton propagators. Note that in the corresponding approach to the conductivity of metals, the relevant two-particle quantity is analogous to Eq. (5), upon summation over both incoming and outgoing wave vector indices.[11,14] Therefore, the perturbation approach applies in an analogous way to our case. The diagrammatic expansion of the scattering matrix corresponding to Eq. (5) is depicted in Fig. 3(a). Here, the single horizontal lines represent configuration-averaged single-exciton propagators $\langle \mathcal{G}^{\pm}(\mathbf{k},\mathbf{k}',\omega)\rangle = G^{\pm}(\mathbf{k},\omega)\,\delta_{\mathbf{k},\mathbf{k}'}$, and the dashed lines denote the potential correlation function in wave vector space, $\sigma^2 f_{\mathbf{q}}$. Intermediate wave vectors have to be summed over as usually.

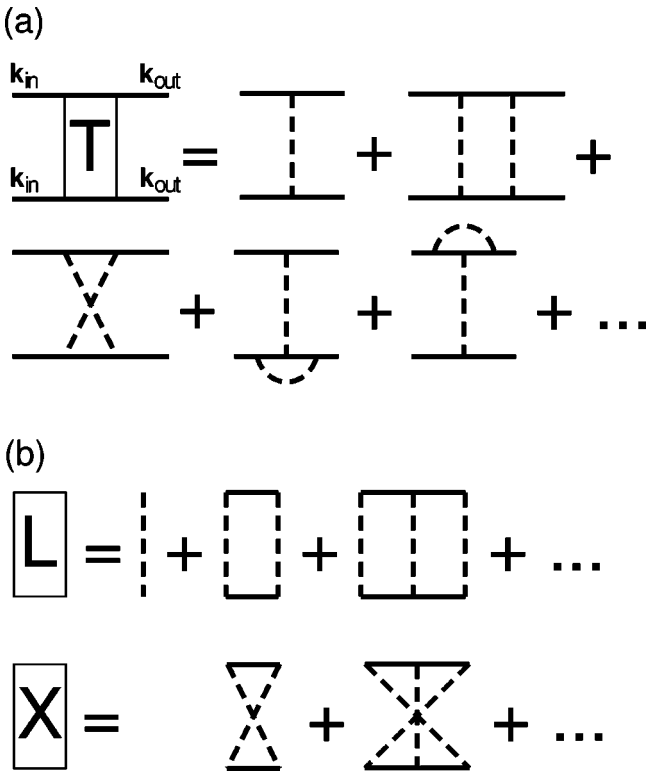

FIG. 3. (a) Diagrams of the perturbation theory for the RRS intensity (up to second order). In each diagram, upper (lower) horizontal lines represent retarded (advanced) one-particle propagators, and the dashed lines are the potential correlation function $\sigma^2 f_{\mathbf{q}}$. Each propagator depends on ω and the $\mathbf{k}$ dependence is indicated explicitly only in the diagram on the left-hand side. (b) Perturbation expansion of the ladder and maximally crossed contributions to the T matrix, $T=L+X$.

When describing localization,[14] the most relevant class of diagrams is represented by two infinite sums consisting of all the ladder and maximally crossed diagrams, as depicted in Fig. 3(b). Correspondingly, the total T matrix is given by

$$T(\mathbf{k}_{in},\mathbf{k}_{out},\omega)=L(\mathbf{k}_{in},\mathbf{k}_{out},\omega)+X(\mathbf{k}_{in},\mathbf{k}_{out},\omega). \quad (6)$$

In a more complete derivation of the diagrammatic approach to EBS,[15] we demonstrate that the applicability of the approximation (6) depends on the form adopted for the single-particle propagator used in the perturbation expansion and, in particular, on the exciton homogeneous broadening γ. We prove that, although in the perturbation theory the backscattering peak approaches a δ function for $\gamma\rightarrow 0$, it is enough to assume a value of γ as small as one tenth of the exciton linewidth to obtain an excellent agreement between the perturbation theory and the exact numerical result. Based

on these considerations and having adopted a finite value of γ in the present calculations, we suggest the following simple expression for the T matrix:

$$T(\mathbf{k}_{in},\mathbf{k}_{out},\omega)=\frac{1+\alpha}{\Gamma^2}+\frac{\alpha}{(\mathbf{k}_{in}+\mathbf{k}_{out})^2+\Gamma^2}. \qquad (7)$$

The functional form of this expression derives from the analytical result of the perturbation approach applied to the one-dimensional case with spatially uncorrelated disordered potential.[15] In particular, the first and second terms on the right side of Eq. (7) correspond to the ladder and maximally crossed series, respectively, and the 1 appears since L contains a first order diagram which has no counterpart in X. This first order diagram plays here a role analogous to the single-scattering paths mentioned above in the case of light scattering in diffuse media. We notice that the ladder contribution is $\mathbf{k}$ independent, while the maximally crossed term is peaked at the EBS wave vector. In 1D perturbation theory for the spatially uncorrelated case, the quantities α and Γ are well defined functions of ω and the homogeneous exciton broadening γ. In the present two-dimensional spatially correlated situation, however, Eq. (7) should be considered only as a phenomenological expression, with α and Γ being two fit parameters. The fit of Eq. (7) to the numerically computed I_D is plotted in Fig. 2(b) as a dashed line. The δ-like reflected contribution to the scattered intensity has intentionally been omitted in the analytical approximation. It would correspond to the zeroth order diagram of two disconnected lines, $G^+(\mathbf{k}_{in},\omega)G^-(\mathbf{k}_{in},\omega)\delta_{\mathbf{k}_{in},\mathbf{k}_{out}}$, not included in the analysis of Fig. 3(a). We notice that the four propagators, by which the T matrix has to be multiplied to obtain the scattered intensity according to Fig. 3(a), are mainly responsible for the dispersion ring in the scattered intensity. They depend on the absolute value of $\mathbf{k}$ only and are thus canceled in the ratio Eq. (4). The success in reproducing our numerical results suggests that Eq. (7) could be used to model the proposed measurement.

In conclusion, we have presented numerical results of frequency- and angle-resolved RRS, based on an existing model of the microscopic exciton polarization in a quantum well with in-plane disorder. We demonstrate a sizeable enhancement of the backscattered light intensity for realistic values of the exciton and disorder parameters. An experimental verification of our prediction would provide the first evidence of disorder-induced EBS in semiconductor heterostructures. We propose a differential measurement in which the EBS shows up clearly, and derive a simple analytical expression which could be used to fit the outcome of forthcoming experiments.

[1] H. Wang, J. Shah, T. C. Damen, and L. N. Pfeiffer, Phys. Rev. Lett. **74**, 3065 (1995).
[2] S. Haacke, R. A. Taylor, R. Zimmermann, I. Bar-Joseph, and B. Deveaud, Phys. Rev. Lett. **78**, 2228 (1997).
[3] M. Gurioli, F. Bogani, S. Ceccherini, and M. Colocci, Phys. Rev. Lett. **78**, 3205 (1997).
[4] D. Birkedal and J. Shah, Phys. Rev. Lett. **81**, 2372 (1998).
[5] M. Woerner and J. Shah, Phys. Rev. Lett. **81**, 4208 (1998).
[6] N. Garro, L. Pugh, R. T. Phillips, V. Drouot, M. Y. Simmons, B. Kardynal, and D. A. Ritchie, Phys. Rev. B **55**, 13 752 (1997); N. Garro, M. J. Snelling, S. P. Kennedy, R. T. Phillips, and K. H. Ploog, *ibid.* **60**, 4497 (1999).
[7] W. Langbein, J. M. Hvam, and R. Zimmermann, Phys. Rev. Lett. **82**, 1040 (1999).
[8] V. Savona and R. Zimmermann, Phys. Rev. B **60**, 4928 (1999).
[9] V. Savona, S. Haacke, and B. Deveaud, Phys. Rev. Lett. **84**, 183 (2000).
[10] M. P. Van Albada and A. Lagendijk, Phys. Rev. Lett. **55**, 2692 (1985); P.-E. Wolf and G. Maret, *ibid.* **55**, 2696 (1985); E. Akkermans, P.-E. Wolf, and R. Maynard, *ibid.* **56**, 1471 (1986); I. Freund, M. Rosenbluh, R. Berkovits, and M. Kaveh, *ibid.* **61**, 1214 (1988); G. Labeyrie, F. de Tomasi, J.-C- Bernard, C. A. Müller, C. Miniatura, and R. Kaiser, *ibid.* **83**, 5266 (1999).
[11] B. Kramer and A. MacKinnon, Rep. Prog. Phys. **56**, 1469 (1993).
[12] E. Hanamura, Phys. Rev. B **39**, 1152 (1989).
[13] Q. Wu, R. D. Grober, D. Gammon, and D. S. Katzer, Phys. Rev. Lett. **83**, 2652 (1999).
[14] D. Vollhardt and P. Wölfle, Phys. Rev. B **22**, 4666 (1980); D. Vollhardt and P. Wölfle, in *Electronic Phase Transitions*, edited by W. Hanke and Yu. V. Kopaev (North-Holland, Amsterdam, 1992).
[15] V. Savona, E. Runge, and R. Zimmermann (unpublished).